HOKKAIDO UNIVERSITY

Title	Degenerative and regenerative features of myofibers differ among skeletal muscles in a murine model of muscular dystrophy
Author(s)	Ikeda, Teppei; Ichii, Osamu; Otsuka-Kanazawa, Saori et al.
Citation	Journal of Muscle Research and Cell Motility, 37(4-5), 153-164 https://doi.org/10.1007/s10974-016-9452-6
Issue Date	2016-10
Doc URL	https://hdl.handle.net/2115/67282
Rights	The final publication is available at link.springer.com
Type	journal article
File Information	J Muscle Res Cell Motil v.37(4-5) p.153-164.pdf

Hokkaido University Collection of Scholarly and Academic Papers : HUSCAP

Degenerative and regenerative features of myofibers differ among skeletal muscles in a murine model of muscular dystrophy

Teppei Ikeda, Osamu Ichii, Saori Otsuka-Kanazawa, Teppei Nakamura, Yaser Hosny Ali Elewa, Yasuhiro Kon*

Laboratory of Anatomy, Department of Biomedical Sciences, Graduate School of Veterinary Medicine, Hokkaido University, Sapporo 060-0818, Japan

***Corresponding author:** Yasuhiro Kon, DVM, PhD,

Laboratory of Anatomy, Department of Biomedical Sciences, Graduate School of Veterinary Medicine, Hokkaido University, Kita 18, Nishi 9, Kita-ku, Sapporo 060-0818, Japan.

Email: y-kon@vetmed.hokudai.ac.jp.

Tel: +81-11-706-5187

Fax: +81-11-706-5189

Acknowledgments

This study was supported by JSPS KAKENHI Grant Number 15J01551.

Abstract

Skeletal muscle myofibers constantly undergo degeneration and regeneration. Histopathological features of 6 skeletal muscles (cranial tibial [CT], gastrocnemius, quadriceps femoris, triceps brachii [TB], lumbar longissimus muscles, and costal part of the diaphragm [CPD]) were compared using C57BL/10ScSn-*Dmd*^{mdx} (mdx) mice, a model for muscular dystrophy versus control, C57BL/10 mice. Body weight and skeletal muscle mass were lower in mdx mice than the control at 4 weeks of age; these results were similar at 6–30 weeks. Additionally, muscular lesions were observed in all examined skeletal muscles in mdx mice after 4 weeks, but none were noted in the controls. Immunohistochemical staining revealed numerous paired box 7-positive satellite cells surrounding the embryonic myosin heavy chain-positive regenerating myofibers, while the number of the former and staining intensity of the latter decreased as myofiber regeneration progressed. Persistent muscular lesions were observed in skeletal muscles of mdx mice between 4–14 weeks of age, and normal myofibers decreased with age. Number of muscular lesions was lowest in CPD at all ages examined, while the ratio of normal myofibers was lowest in TB at 6 weeks. In CT, TB, and CPD, Iba1-positive macrophages, the main inflammatory cells in skeletal muscle lesions, showed a significant positive correlation with the appearance of regenerating myofibers. Additionally, B220-positive B-cells showed positive and negative correlation with regenerating and regenerated myofibers, respectively. Our data suggest that degenerative and regenerative features of myofibers differ among skeletal muscles and that inflammatory cells are strongly associated with regenerative features of myofibers in mdx mice.

Key words: muscular dystrophy, mdx mouse, skeletal muscle remodeling, inflammation, triceps brachii, costal part of the diaphragm

Abbreviations: CT, cranial tibial muscle; CPD, costal part of the diaphragm; GA, gastrocnemius muscle; HE, hematoxylin-eosin; LL, lumbar longissimus muscle; MRF, myogenic regulatory factor; MT, Masson's trichrome stain; QR, quadriceps femoris muscle; TB, triceps brachii muscle

INTRODUCTION

Skeletal muscles have high regenerative ability and satellite cells, also known as myogenic precursor cells, play a key role in muscle regeneration (Chargé and Rudnicki 2004). Skeletal muscle remodeling, which involves degeneration and regeneration of myofibers, is a constant process in all animals. Aging, metabolic diseases, hereditary muscle diseases and neuromuscular diseases can affect the processes involved in skeletal muscle remodeling, which lead to breakdown and atrophy of skeletal muscle. Muscle repair is a multistep process that includes myofiber degeneration and regeneration (Le Grand and Rudnicki 2007; Ten Broek et al. 2010; Tsivitse 2010). Following damage to myofibers, satellite cells are activated and proliferate to give rise to a population of transient, amplifying myogenic cells called myoblasts, which express myogenic regulatory factors (MRFs) such as myogenic differentiation 1 and myogenic factor 5. Myoblasts subsequently express another MRF called myogenin, commit to terminal differentiation, and fuse to reconstruct their host myofibers or to generate new myofibers and repair damaged tissue (Tedesco et al. 2010).

Duchenne muscular dystrophy (DMD), the most common and severe type of muscular dystrophy in humans, is an X-linked, recessive, lethal muscle wasting disease affecting approximately 1 in 3,500 boys (Emery 1989). It is caused by mutations in the *DMD* gene, located on the X chromosome, which codes for dystrophin, a membrane-associated structural protein. Homologues of *DMD* have been identified in several animals including dogs (Cooper et al. 1988), cats (Carpenter et al. 1989) and mice (Bulfield et al. 1984; Pastoret and Sebille 1995). C57BL/10ScSn-Dmd^{mdx} (mdx) mice do not produce dystrophin, due to a point-mutation in *Dmd*. Though these mice do not represent a complete phenotypic model of DMD in humans, they have been used as a representative animal model of DMD (Bulfield et al. 1984). These mice show pathological changes in skeletal muscles, characterized by necrosis of skeletal muscle fibers accompanied by regeneration (Bulfield et al. 1984; Pastoret and Sebille 1995; Boland et al. 1995).

It has been observed that the pathological features of DMD differ among different types of skeletal muscles. Skeletal muscles of the thoracic esophagus show no necrosis and no regenerating fibers in mdx

mice (Boland et al. 1995). However, large numbers of necrotic myofibers have been seen between 3 and 4 weeks of age in limb muscle (Shavlakadze et al. 2004), followed by regeneration of myofibers by 6 to 12 weeks of age (McGeachie et al. 1993). In contrast to the limb, muscles of the diaphragm show progressive degeneration of myofibers (Stedman et al. 1991). Therefore, a comparison of histopathological changes among the muscles of mdx mice would be useful to better understand the pathological characteristics of DMD (Louboutin et al. 1993; Pastoret and Sebille 1995; Boland et al. 1995).

Inflammation is a crucial process that is thought to both, exacerbate damage and necrosis as well as promote regeneration in skeletal muscles. Inflammatory cells, especially neutrophils and macrophages, mediate necrosis of muscle cells via oxidative damage both, *in vitro* (Pizza et al. 2001; McLoughlin et al. 2003; Nguyen and Tidball 2003) and *in vivo* (Pizza et al. 2005; Cheung and Tidball 2003; Nguyen and Tidball 2003), with macrophages also performing their principal role of phagocytizing necrotic cells (Almekinders and Gilbert 1986; Robertson et al. 1993; Lescaudron et al. 1999; Merly et al. 1999; Mojumdar et al, 2014). Further, it has been proposed that an excessive inflammatory response can directly damage myofibers under myopathic conditions such as dystrophies or myositis (Porter et al. 2002). Importantly, DNA microarray studies of mdx muscle show that 30% of all differentially expressed genes are associated with inflammation (Porter et al. 2002; Porter et al. 2004; Tidball 2005).

In this study, we demonstrated that degenerative and regenerative features of myofibers differ among skeletal muscles in mdx mice, and that these differences are associated with immune cell infiltration into the skeletal muscle lesions. Each skeletal muscle in the adult mammalian body has a different character based on anatomical, physiological, and/or mechanical factors such as exercise load and posture of the animal. The findings of this study shed light on the process of muscle remodeling and the pathological differences among different types of skeletal muscles in DMD.

MATERIALS AND METHODS

Experimental animals

Animal experimentation was approved by the Institutional Animal Care and Use Committee of the Graduate School of Veterinary Medicine, Hokkaido University (approval No. 13-0032). Male, mdx mice were purchased from Central Institute for Experimental Animals (Kanagawa, Japan) and control, male C57BL/10SnSlc (B10) mice were purchased from Japan SLC (Shizuoka, Japan). Mice were housed in the animal facility of Graduate School of Veterinary Medicine, Hokkaido University. The body weight of B10 and mdx mice was measured at 1 (B10, mdx; n = 4, 19, respectively), 2 (n = 4, 17), 3 (n = 4, 17), 4 (n = 10, 17), 6 (n = 5, 12), 8 (n = 5, 11), 14 (n = 5, 10), and 30 (n = 4, 4) weeks of age. Skeletal muscles were harvested at 4 (n = 4), 6 (n = 4), and 14 (n = 4) weeks of age. The genotype of mdx mice was analyzed by TaqMan PCR (Applied Biosystems, Foster, CA, USA) targeting a point mutation in the *DMD* gene. Experimental animals were handled in accordance with the Guide for the Care and Use of Laboratory Animals, Graduate School of Veterinary Medicine, Hokkaido University (approved by the Association for Assessment and Accreditation of Laboratory Animal Care International).

Tissue preparation and microscopic observation

The caudal vena cava was cut under deep anesthesia by an intraperitoneal injection (0.012–0.015 ml/g of body weight) of 2.5% Avertin, while 4% paraformaldehyde was perfused from the left ventricle. Six skeletal muscles (cranial tibial muscle, CT; gastrocnemius muscle, GA; quadriceps femoris muscle, QR; triceps brachii muscle, TB; lumbar longissimus muscle, LL; and costal part of the diaphragm, CPD) were collected. The muscles from the left side of the body were fixed in 10% neutral buffer formalin for 32–48 hours for morphological examination, while those from the right side of the body were fixed in 4% paraformaldehyde for 18–24 hours for immunohistochemical staining. After fixation, specimens were dehydrated in graded alcohol and embedded in paraffin. Subsequently, 2-μm-thick paraffin sections of each skeletal muscle were deparaffinized, rehydrated, stained with hematoxylin-eosin (HE) and Masson's

trichrome stain (MT), and observed under a light microscope.

Immunohistochemistry

Immunohistochemical staining for embryonic myosin heavy chain (eMyHC), paired box 7 (PAX7), Gr1 (Ly-6G), Iba1, B220, and CD3 was performed using 3-µm-thick paraffin sections to detect regenerating myofibers, satellite cells, granulocytes, pan-macrophages (including M1/M2 macrophages; Pierezan et al, 2014), B-cells, and pan T-cells, respectively. The paraffin sections were deparaffinized and antigen was retrieved. After cooling, slides were soaked in methanol containing 3% H_2O_2 for 20 minutes at room temperature to remove internal peroxidase. After washing, sections were blocked with mouse blocking reagent (Nichirei, Tokyo, Japan) for eMyHC and PAX7, and with 10% normal goat serum (Nichirei, Tokyo. Japan) for Gr1, Iba1, B220, and CD3, for 60 minutes at room temperature and incubated with primary antibodies overnight, at 4°C. After washing thrice with phosphate-buffered saline, sections were incubated with secondary antibodies for 30 minutes at room temperature, washed, and incubated with streptavidin-biotin complex (SABPO® kit; Nichirei, Tokyo, Japan) for 30 minutes. The sections were then incubated with 3,3′-diaminobenzidine tetrahydrochloride-H_2O_2 solution. Finally, the sections were lightly counterstained with hematoxylin. Details of the antigen retrieval method as well as the source and dilution of the antibodies are listed in Table 1.

Histoplanimetry

Quantitative analysis of degenerative and regenerative myofibers was performed using ImageJ (http://rsb.info.nih.gov/ij/) software, as previously described (Pastoret and Sebille 1995). Briefly, opaque as well as faintly colored fibers, frequently filled with phagocytes were classified as degenerating myofibers. Small fibers in which, the cytoplasm takes on a uniformly bluish color, with central vesicular nuclei were classified as regenerating myofibers. Fibers with non-peripheral nuclei and eosinophilic cytoplasm were classified as regenerated myofibers. All others were classified as normal myofibers. All

myofibers in transverse sections of each skeletal muscle were counted (at least 2,000 myofibers per specimen) and classified into 1 of the 4 types of myofibers described above. Based on immunohistochemical staining, the number of Gr1-, Iba1-, B220-, and CD3-positive cells in each skeletal muscle was counted, and the total area of transverse sections of each skeletal muscle was then measured. Finally, the number of immune-positive cells was divided by the total area of transverse sections of each skeletal muscle, and these values were expressed as cell number per unit area (number/mm^2).

Statistical analysis

All numerical results are presented as mean ± standard error (SE) and analyzed using non-parametric methods. The Mann-Whitney *U*-test was used to compare 2 groups ($P < 0.05$). The Kruskal-Wallis test was used to compare 3 or more groups, and multiple comparisons were performed using Scheffé's method when a significant difference was observed ($P < 0.05$). Correlation between myofibers exhibiting histopathological changes and immune cell numbers in the skeletal muscle lesions was analyzed by Spearman's correlation coefficient test (ρ) ($P < 0.05$).

Results

Body weight and skeletal muscle mass in mdx and B10 mice

Changes in body weight and skeletal muscle mass were compared between mdx and B10 mice from 1 to 30 weeks of age. Body weight was similar between the 2 groups up to 3 weeks of age. However, at 4 weeks, the body weight of mdx mice was significantly lower than that of B10 mice (Figure 1A). From 6 weeks onwards, body weight was similar again between the two groups. Gross anatomical and histological examination at 4 weeks of age revealed that the muscle mass of mdx mice was markedly lower compared to that of B10 mice. Accordingly, the skeletal muscle area in the transverse sections of all examined skeletal muscles was reduced in mdx mice than in B10 mice at 4 weeks of age (Figure 1B). Muscular histopathological changes, such as degenerative and atrophied myofibers, were widely but focally observed in mdx mice, but not in B10 mice (Figure 1B). However, at 6 weeks of age, the skeletal muscle areas of mdx mice seemed to increase to almost equal levels to those in B10 mice (Figure 1C). In mdx mice, myofibers with non-peripheral nuclei occupied the observed area at 6 weeks (Figure 1C). In addition to the results of body weight change and muscle features (Figure 1), we considered previous reports (Shavlakadze et al. 2004; McGeachie et al. 1993) and examined ages and divided the mdx mouse group into the muscle degenerative phase (4 weeks of ages), muscle regenerative phase (6 weeks onward), and the sexually matured and muscle regenerated phase (14 weeks).

Histopathological features of skeletal muscle in mdx and B10 mice

We analyzed the histopathological changes shown in Figure 1B in more detail. As shown in Figure 2, B10 mice showed no histological changes in any of the examined muscles. In mdx mice, on the other hand showed no histopathological changes in skeletal muscles at 2 weeks of age, and very few changes at 3 weeks (data not shown). However, severe histopathological changes were observed from 4 weeks of age (Figure 2). Muscular lesions were observed focally in all mdx mice at all examined ages. These lesions consisted of 3 types of myofibers: degenerative myofibers (arrows in Figure 2), regenerating myofibers

(small arrowheads in Figure 2), and regenerated myofibers (large arrowheads in Figure 2). Although these muscular lesions were observed in all examined muscles of mdx mice, the number of degenerative myofibers tended to be lower in CPD compared to other skeletal muscles (Figure 2). These results suggest that the progression of histopathological changes in mdx mice may differ among skeletal muscles.

To further investigate regenerative features of myofibers in mdx mice, immunohistochemical staining was carried out. Numerous PAX7-positive muscle satellite cells surrounded eMyHC-positive regenerating myofibers in skeletal muscles of mdx mice (Figure 3A–F), and the number of the former and the staining intensity of the latter gradually decreased with the progression of myofiber regeneration (Figure 3A–C and G–L).

Histopathological changes in different skeletal muscles of mdx mice

To compare the muscular lesions among examined skeletal muscles in mdx mice, we compared the ratio of the number of fibers classified as normal, degenerative, and centronucleated (regenerating/regenerated) to the total number of muscle fibers in each skeletal muscle examined (Figure 4). Although all examined skeletal muscles contained muscular lesions during the observation period, the ratio of each type of myofiber differed among skeletal muscles. The ratios of normal and degenerative myofibers were larger and smaller, respectively, in CPD compared with other muscles at 4 weeks of age (Figure 4A and B). The ratios of normal myofibers also tended to be larger in CPD than in the other muscles at 6 and 14 weeks of age (Figure 4A). Further, the ratio of centronucleated myofibers, indicating regenerating or regenerated myofibers, tended to be smaller in CPD than in the other muscles (Figure 4C). Significant differences between CPD and the other muscles were observed in terms of ratio of regenerated myofibers and that of regenerating myofibers (Figure 4D and E). At 6 weeks of age, the ratio of normal myofibers was significantly smaller in TB as compared to that in CT, GA, and CPD. In addition to these variations among different skeletal muscles, significant differences were noted in muscular lesions with respect to ratios, within the same skeletal muscle. The ratio of normal and

centronucleated myofibers, especially regenerated myofibers, were smaller and larger, respectively, at 14 as compared to 4 weeks of age, in all examined muscles (Figure 4A, C, and E). These results indicate that the pathological features of muscular lesions differed among skeletal muscles and with age. In particular, CPD and TB tended to show milder and severer lesions, respectively, compared with other examined skeletal muscles, in mdx mice.

Distribution of immune cells in skeletal muscle lesions

Since morphological analysis using HE and/or MT staining indicated the presence of macrophages and granulocytes (especially neutrophils) in the muscular lesions (Figure 2 and 3D), the distribution of immune cells was analyzed by immunohistochemistry. Histopathological analyses described above indicated that TB and CPD showed different features of muscular lesions compared with the other skeletal muscles examined. Therefore, immunohistochemical analysis was performed for TB, CPD, and CT muscles, where CT served as control. Immunohistochemical staining revealed the presence of Iba1-, Gr1-, B220-, and CD3-positive cells in the skeletal muscle lesions of mdx mice (Figure 5A–D). All positive reactions were counted and normalized by the area of each skeletal muscle. Iba1- and Gr1-positive cells were high in TB at 4 weeks of age and low in TB and CPD at 14 weeks of age, but no significant differences were noted in any skeletal muscle with respect to age (Figure 5E and F). B220-positive cells in CT and TB, whereas CD3-positive cells in TB were significantly higher at 4 weeks of age as compared to those at 6 and 14 weeks of age (Figure 5G and H). A significant difference in the number of immune cells in the examined skeletal muscles at the same age was observed only in CD3 at 14 weeks of age. CPD showed a large number of CD3-positive cells compared to CT, at 14 weeks of age (Figure 5H). The number of Iba1-positive cells was the highest of the 4 immune cells examined, in all skeletal muscles at the same age (Figure 5E).

Correlation between histopathological changes in skeletal muscles and immune cell numbers

233 As shown in Figure 6, a significant correlation was observed between Iba1-positive cells and
234 regenerating myofibers (Figure 6B), between Gr1 and regenerated myofibers (Figure 6F), and between
235 B220-positive cells and regenerated myofibers (Figure 6I).
236

Discussion

The present study demonstrated that degenerative and regenerative features of myofibers differ among skeletal muscles in mdx DMD model mice. Body weight of mdx mice was significantly lower than that of B10 mice at 4 weeks of age, but was similar at 6 weeks. Myofiber necrosis has been previously observed in mdx mice at 3 weeks of age, followed by myofiber regeneration (Coulton et al. 1988; McGeachie et al. 1993; Grounds and Torrisi 2004). Additionally, a large number of necrotic myofibers have been observed between 3 and 4 weeks of age in CT muscle (Shavlakadze et al. 2004). After onset of acute myofiber necrosis, degeneration of skeletal muscle decreases accompanied by regeneration of myofibers and is at a low level by 6 to 12 weeks of age (McGeachie et al. 1993). In the present study, the skeletal muscle area was smaller in mdx mice than in B10 mice in transverse sections of all examined skeletal muscles at 4 weeks of age, but was comparable at 6 weeks. This recovery of the skeletal muscle area is thought to be the result of acute regeneration of myofibers. Further, Pastoret and Sebille (1995) compared the body weight and CT muscles of mdx and B10 mice from 2 to 104 weeks of age, resulting that mdx mice showed higher body weight than B10 mice from 13 to 26 weeks of age, due to hypertrophy of mdx skeletal muscle. Therefore, hypertrophy of skeletal muscle could be one of the morphological features of myofiber regeneration in mdx mice. A significant difference in body weight of mdx and B10 mice at 4 weeks of age was observed in the present study, which may be due to degeneration of skeletal muscles in mdx mice.

From 4 weeks of age onwards, skeletal muscle lesions containing degenerating, regenerating, or regenerated myofibers were observed in mdx mice. Different muscles have been analyzed in mdx mice after exercise (Weller et al. 1990; Brussee et al. 1997; Granchelli et al. 2000; De Luca et al. 2005), administration of drugs (Hodgetts et al. 2006), engraftment of somatic cells (Hindi et al. 2013; Boldrin et al. 2015), and gene modification (Li et al. 2009; Heydemann et al. 2012). The results obtained and the skeletal muscles analyzed are different in these previous reports. The present study compared 6 skeletal muscles: CT, GA, QR, TB, LL, and CPD at 4, 6 and 14 weeks of age and found that the extent

of degeneration and regeneration differs among skeletal muscles with age, in mdx mice. CPD tended to show less pathological changes than other skeletal muscles in mdx mice during the examined period. A similar observation was reported by Louboutin et al., who demonstrated that histopathological changes in the mdx diaphragm are rare before 25 days of age, whereas the degeneration of myofibers begins at 21-25 days of age in the hind limb muscles (extensor digitorum longus: EDL, CT, and soleus). Additionally, regenerating fibers with central nuclei were fewer in the diaphragm than in hind limb muscles during the observation period of 30 to 270 days of age (Louboutin et al. 1993). Boland et al. also showed a lower number of myofibers with central nuclei and a higher number of myofibers with peripheral nuclei in the diaphragm than in CT and rectus abdominis muscles of mdx mice during 12-18 months of age (Boland et al., 1995). Although the pathological implications of nuclear position in muscle diseases might be debatable, these data and a recent study showed skeletal muscle fibers with central nuclei as regenerated myofibers (Boldrin et al., 2015); thus we considered that central nuclei could be used as a marker of regeneration. In the present study, CPD tended to show a higher ratio of normal fiber as compared to the other skeletal muscles, especially at 4 weeks of age. Regeneration of myofibers begins after degeneration and the number of regeneration fibers increased clearly with age in CPD of mdx mice. This indicates that CPD shows late-onset degeneration of myofibers. However, Louboutin *et al*. also showed that fibrosis, occasionally including adipose tissue replacement, is observed at 270 days of age in the diaphragm, but was less-frequent in hind limb muscles (Louboutin et al. 1993), indicating that CPD might have lower regenerative ability as compared to other skeletal muscles. Fiber-type transition is a pathological response against contraction-induced injury in DMD (Gehrig et al. 2010). However, Schneider et al. observed the diaphragm as a severely affected muscle in DMD and examined the fiber-type switch compared with quadriceps (a fast-twitch muscle) and soleus (a slow-twitch muscle) in 2-month-old mouse models of DMD. They reported fiber-type transition from fast-fiber (type 2b) to slow-fiber (type 1 and type 2a) in all of the 3 muscles; however, type 1 MyHC and eMyHC are not co-expressed, suggesting that regeneration

287 and fiber-type switch are two independent mechanisms in the dystrophic muscles (Schneider et al.,
288 2013).

289 In addition, the present study shows that increased muscular lesions are observed in TB compared
290 to the other skeletal muscles at 6 weeks of age. Brussee *et al.* also reported that TB of mdx mice
291 showed more atrophied myofibers than CT, EDL, soleus, GA, biceps brachii, and diaphragm muscles
292 under sedentary conditions (Brussee et al. 1997). Interestingly, they also showed that the severity of
293 muscle damage among skeletal muscles differed after 3 days of downhill running exercise compared to
294 sedentary conditions (Brussee et al. 1997). The present study shows that the degree of degeneration and
295 regeneration, involving damage to myofibers or subsequent reactions of muscular satellite cells or
296 myoblasts, differs among skeletal muscles, which may have an effect on the phenotypes of mdx mice.

297 The difference in muscle pathological features in mdx mice has been examined in several previous
298 reports (Louboutin et al. 1993; Brussee et al. 1997); however, their inflammatory features in different
299 muscles are scarcely addressed. The present study demonstrated that Iba1-positive macrophages are the
300 major inflammatory cells in skeletal muscle lesions that positively correlate with the number of
301 regenerating myofibers, whereas Gr1-positive granulocytes, mainly neutrophils, negatively correlate
302 with regenerated myofibers in mdx mice. After muscle injury caused by trauma such as extensive
303 physical activity, or by innate genetic defects, inflammatory cells such as neutrophils and macrophages
304 infiltrate into the lesions (Belcastro et al. 1996). Necrosis of myofibers is the initial event in skeletal
305 muscle degeneration, accompanied by the activation of mononucleated cells, principally inflammatory
306 and myogenic cells. Neutrophils are the first inflammatory cells to infiltrate the injured muscle, with a
307 significant increase in their numbers as early as 1–6 h after myotoxin- or exercise-induced muscle
308 damage (Orimo et al. 1991; Fielding et al. 1993). Some reports revealed that prevention of neutrophil
309 infiltration after injury reduces force deficits and histological damage to muscle fibers (Walden et al.
310 1990; Brickson et al. 2003; Pizza et al. 2005; Lockhart and Brooks 2008), suggesting that neutrophils
311 contribute to muscle fiber damage. In the present study, although neutrophils did not show a correlation

312 with degenerating myofibers, a negative correlation with regenerated myofibers was noted, indicating
313 that neutrophils decrease with progression of regeneration. After neutrophil infiltration, macrophages
314 become the predominant inflammatory cell type within the site of injury (Orimo et al. 1991; Tidball
315 2005). Macrophages, especially the M2-type, infiltrate the injured site to phagocytose cellular debris
316 and may affect other aspects of muscle regeneration by activating myogenic cells (Almekinders and
317 Gilbert 1986; Robertson et al. 1993; Lescaudron et al. 1999; Merly et al. 1999). Muscle degeneration is
318 followed by the activation of a muscle repair process. Myogenic cells differentiate and fuse to existing
319 damaged fibers for repair or to one another for new myofiber formation (Snow 1977; Snow 1978; Darr
320 and Schultz 1987). Muscle regeneration is slower in older animals, which coincides with weakened
321 phagocytosis activity by inflammatory cells (Zacks and Sheff MF 1982; Grounds 1987). In addition,
322 mouse strains with slower rates of phagocytic removal of muscle debris show slower rates of muscle
323 regeneration (Grounds 1987). No significant difference in Iba1- and Gr1-positive cell infiltration was
324 observed among muscles in the present study; however, many studies support the hypothesis that
325 phagocytosis is a necessary feature of muscle repair, and that macrophages and neutrophils play an
326 important role in this process.

327 The present study also revealed that B220-positive, B cells were negatively correlated with
328 regenerated myofibers. Several studies suggest that B- and T-cells contribute to the development of
329 muscle fibrosis in aged (> 12 months) SCID-mdx (Farini et al. 2007) and nu/nu-mdx mice (Morrison et
330 al. 2000). The absence of B and T cells results in reduced fibrosis, accompanied by a reduction of
331 transforming growth factor-β1 (Farini et al. 2007). In the present study, although the number of B
332 and/or T cells was significantly lower than that of macrophages (data not shown) and slightly lower
333 than that of neutrophils, in all examined skeletal muscles at each age, numbers of both B and T cells
334 were significantly higher in TB at 4 weeks of age compared to that at 6 and 14 weeks of age, suggesting
335 their importance in the early stages of muscular dystrophy in mdx mice.

336 In conclusion, the degenerative and regenerative features of myofibers in mdx mice differ among

skeletal muscles. Inflammatory cells, especially phagocytes and B cells, are strongly associated with the regenerative features of myofibers. Though the triggers for these pathological differences are unknown, anatomical, physiological, and/or mechanical factors such as exercise load may affect these differences in remodeling processes among examined skeletal muscles. Further research involving the study of muscle cells using cell-specific markers and quantification of MRFs in skeletal muscles, is required to further understand muscular remodeling.

Authors' contributions

YK conceptualized the study. TI, OI, TN, YE, and YK designed the experiments. TI performed the experiments and analyzed the data. TI, OI, and YK drafted the manuscript.

Disclosures

The authors declare no conflicts of interest.

References

Almekinders LC, Gilbert JA (1986) Healing of experimental muscle strains and the effects of nonsteroidal anti-inflammatory medication. Am J Sports Med 14:303–308.

Belcastro AN, Arthur GD, Albisser TA, Raj DA (1996) Heart, liver, and skeletal muscle myeloperoxidase activity during exercise. J Appl Physiol (1985) 80(4):1331–1335.

Boland B, Himpens B, Denef JF, Gillis JM (1995) Site-dependent pathological differences in smooth muscles and skeletal muscles of the adult mdx mouse. Muscle Nerve 18(6):649–657.

Boldrin L, Zammit PS, Morgan JE (2015) Satellite cells from dystrophic muscle retain regenerative capacity. Stem Cell Res 14(1):20–29. doi: 10.1016/j.scr.2014.10.007

Brickson S, Ji LL, Schell K, Olabisi R, St Pierre Schneider B, Best TM (2003) M1/70 attenuates blood-borne neutrophil oxidants, activation, and myofiber damage following stretch injury. J Appl Physiol (1985) 95(3):969–976.

Brussee V, Tardif F, Tremblay JP (1997) Muscle fibers of mdx mice are more vulnerable to exercise than those of normal mice. Neuromuscul Disord 7(8):487–492.

Bulfield G, Siller WG, Wight PA, Moore KJ (1984) X chromosome-linked muscular dystrophy (mdx) in the mouse. Proc Natl Acad Sci U S A 81(4):1189–1192.

Carpenter JL, Hoffman EP, Romanul FC, Kunkel LM, Rosales RK, Ma NS, Dasbach JJ, Rae JF, Moore FM, McAfee MB, Pearce LK (1989) Feline muscular dystrophy with dystrophin deficiency. Am J Pathol 135(5):909–919.

Chargé SB, Rudnicki MA (2004) Cellular and molecular regulation of muscle regeneration. Physiol Rev 84(1):209–238.

Cheung EV, Tidball JG (2003) Administration of the non-steroidal anti-inflammatory drug ibuprofen increases macrophage concentrations but reduces necrosis during modified muscle use. Inflamm Res 52(4):170–176.

Cooper BJ, Winand NJ, Stedman H, Valentine BA, Hoffman EP, Kunkel LM, Scott MO, Fischbeck KH,

376 Kornegay JN, Avery RJ, Williams JR, Schmickel RD, Sylvester JE (1988) The homologue of the
377 Duchenne locus is defective in X-linked muscular dystrophy of dogs. Nature 334(6178):154–156.
378 Coulton GR, Morgan JE, Partridge TA, Sloper JC (1988) The mdx mouse skeletal muscle myopathy: I. A
379 histological, morphometric and biochemical investigation. Neuropathol Appl Neurobiol 14(1):53–70.
380 Darr KC, Schultz E (1987) Exercise-induced satellite cell activation in growing and mature skeletal
381 muscle. J Appl Physiol (1985) 63(5):1816–1821.
382 De Luca A, Nico B, Liantonio A, Didonna MP, Fraysse B, Pierno S, Burdi R, Mangieri D, Rolland JF,
383 Camerino C, Zallone A, Confalonieri P, Andreetta F, Arnoldi E, Courdier-Fruh I, Magyar JP, Frigeri A,
384 Pisoni M, Svelto M, Conte Camerino D (2005) A multidisciplinary evaluation of the effectiveness of
385 cyclosporine a in dystrophic mdx mice. Am J Pathol 166(2):477–489.
386 Emery AE (1989) Clinical and molecular studies in Duchenne muscular dystrophy. Prog Clin Biol
387 306:15–28.
388 Farini A, Meregalli M, Belicchi M, Battistelli M, Parolini D, D'Antona G, Gavina M, Ottoboni L,
389 Constantin G, Bottinelli R, Torrente Y (2007) T and B lymphocyte depletion has a marked effect on the
390 fibrosis of dystrophic skeletal muscles in the scid/mdx mouse. J Pathol 213(2):229–238.
391 Fielding RA, Manfredi TJ, Ding W, Fiatarone MA, Evans WJ, Cannon JG (1993) Acute phase response in
392 exercise. III. Neutrophil and IL-1 beta accumulation in skeletal muscle. Am J Physiol 265(1 Pt 2):R166 –
393 R172.
394 Gehrig SM, Koopman R, Naim T, Tjoakarfa C, Lynch GS (2010) Making fast-twitch dystrophic muscles
395 bigger protects them from contraction injury and attenuates the dystrophic pathology. Am J Pathol
396 176(1):29–33. doi: 10.2353/ajpath.2010.090760
397 Granchelli JA, Pollina C, Hudecki MS (2000) Pre-clinical screening of drugs using the mdx mouse.
398 Neuromuscul Disord 10(4-5):235–239.
399 Grounds MD (1987) Phagocytosis of necrotic muscle in muscle isografts is influenced by the strain, age,
400 and sex of host mice. J Pathol 153(1):71–82.

401 Grounds MD, Torrisi J (2004) Anti-TNFalpha (Remicade) therapy protects dystrophic skeletal muscle
402 from necrosis. FASEB J 18(6):676–682.
403 Heydemann A, Swaggart KA, Kim GH, Holley-Cuthrell J, Hadhazy M, McNally EM (2012) The
404 superhealing MRL background improves muscular dystrophy. Skelet Muscle 2(1):26. doi:
405 10.1186/2044-5040-2-26
406 Hindi SM, Shin J, Ogura Y, Li H, Kumar A (2013) Matrix metalloproteinase-9 inhibition improves
407 proliferation and engraftment of myogenic cells in dystrophic muscle of mdx mice. PLoS One
408 8(8):e72121. doi: 10.1371/journal.pone.0072121
409 Hodgetts S, Radley H, Davies M, Grounds MD (2006) Reduced necrosis of dystrophic muscle by
410 depletion of host neutrophils, or blocking TNFalpha function with Etanercept in mdx mice. Neuromuscul
411 Disord 16(9-10):591–602.
412 Le Grand F, Rudnicki M (2007) Satellite and stem cells in muscle growth and repair. Development
413 134(22):3953–3957.
414 Lescaudron L, Peltékian E, Fontaine-Pérus J, Paulin D, Zampieri M, Garcia L, Parrish E (1999) Blood
415 borne macrophages are essential for the triggering of muscle regeneration following muscle transplant.
416 Neuromuscul Disord 9(2):72–80.
417 Li H, Mittal A, Makonchuk DY, Bhatnagar S, Kumar A (2009) Matrix metalloproteinase-9 inhibition
418 ameliorates pathogenesis and improves skeletal muscle regeneration in muscular dystrophy. Hum Mol
419 Genet 18(14):2584–2598. doi: 10.1093/hmg/ddp191
420 Lockhart NC, Brooks SV (2008) Neutrophil accumulation following passive stretches contributes to
421 adaptations that reduce contraction-induced skeletal muscle injury in mice. J Appl Physiol (1985)
422 104(4):1109–1115. doi: 10.1152/japplphysiol.00850.2007
423 Louboutin JP, Fichter-Gagnepain V, Thaon E, Fardeau M (1993) Morphometric analysis of mdx
424 diaphragm muscle fibers. Comparison with hindlimb muscles. Neuromuscul Disord 3(5-6):463–469.
425 McGeachie JK, Grounds MD, Partridge TA, Morgan JE (1993) Age-related changes in replication of

426 myogenic cells in mdx mice: quantitative autoradiographic studies. J Neurol Sci 119(2):169–179.

427 McLoughlin TJ, Tsivitse SK, Edwards JA, Aiken BA, Pizza FX (2003) Deferoxamine reduces and nitric
428 oxide synthase inhibition increases neutrophil-mediated myotube injury. Cell Tissue Res 313(3):313–319.

429 Merly F, Lescaudron L, Rouaud T, Crossin F, Gardahaut MF (1999) Macrophages enhance muscle
430 satellite cell proliferation and delay their differentiation. Muscle Nerve 22(6):724–732.

431 Morrison J, Lu QL, Pastoret C, Partridge T, Bou-Gharios G (2000) T-cell-dependent fibrosis in the mdx
432 dystrophic mouse. Lab Invest 80(6):881–891.

433 Mojumdar K, Liang F, Giordano C, Lemaire C, Danialou G, Okazaki T, Bourdon J, Rafei M, Galipeau J,
434 Divangahi M, Petrof BJ (2014) Inflammatory monocytes promote progression of Duchenne muscular
435 dystrophy and can be therapeutically targeted via CCR2. EMBO Mol Med 6(11):1476-1492.

436 Nguyen HX, Tidball JG (2003) Expression of a muscle-specific, nitric oxide synthase transgene prevents
437 muscle membrane injury and reduces muscle inflammation during modified muscle use in mice. J Physiol
438 550(Pt 2):347–356.

439 Nguyen HX, Tidball JG (2003) Interactions between neutrophils and macrophages promote macrophage
440 killing of rat muscle cells in vitro. J Physiol 547(Pt 1):125–132.

441 Orimo S, Hiyamuta E, Arahata K, Sugita H (1991) Analysis of inflammatory cells and complement C3 in
442 bupivacaine-induced myonecrosis. Muscle Nerve 14(6):515–520.

443 Pastoret C, Sebille A (1995) Mdx mice show progressive weakness and muscle deterioration with age. J
444 Neurol Sci 129(2):97–105.

445 Pierezan F, Mansell J, Ambrus A, Rodrigues Hoffmann A (2014) Immunohistochemical expression of
446 ionized calcium binding adapter molecule 1 in cutaneous histiocytic proliferative, neoplastic and
447 inflammatory disorders of dogs and cats. J Comp Pathol 151:347-351.

448 Pizza FX, Koh TJ, McGregor SJ, Brooks SV (2001) Muscle inflammatory cells after passive stretches,
449 isometric contractions and lengthening contractions. J Appl Physiol (1985) 92(5):1873–1878.

450 Pizza FX, McLoughlin TJ, McGregor SJ, Calomeni EP, Gunning WT (2001) Neutrophils injure cultured

451 skeletal myotubes. Am J Physiol Cell Physiol 281(1):C335–C341.

452 Pizza FX, Peterson JM, Baas JH, Koh TJ (2005) Neutrophils contribute to muscle injury and impair its
453 resolution after lengthening contractions in mice. J Physiol 562(Pt 3):899–913.

454 Porter JD, Khanna S, Kaminski HJ, Rao JS, Merriam AP, Richmonds CR, Leahy P, Li J, Guo W, Andrade
455 FH (2002) A chronic inflammatory response dominates the skeletal muscle molecular signature in
456 dystrophin-deficient mdx mice. Hum Mol Genet 11(3):263–272.

457 Porter JD, Merriam AP, Leahy P, Gong B, Feuerman J, Cheng G, Khanna S (2004) Temporal gene
458 expression profiling of dystrophin-deficient (mdx) mouse diaphragm identifies conserved and muscle
459 group-specific mechanisms in the pathogenesis of muscular dystrophy. Hum Mol Genet 13(3):257–269.

460 Robertson TA, Maley MA, Grounds MD, Papadimitriou JM (1993) The role of macrophages in skeletal
461 muscle regeneration with particular reference to chemotaxis. Exp Cell Res 207(2):321–331.

462 Schneider JS, Shanmugam M, Gonzalez JP, Lopez H, Gordan R, Fraidenraich D, Babu GJ (2013)
463 Increased sarcolipin expression and decreased sarco(endo)plasmic reticulum Ca2+ uptake in skeletal
464 muscles of mouse models of Duchenne muscular dystrophy. J Muscle Res Cell Motil 34(5-6):349-356.
465 doi: 10.1007/s10974-013-9350-0

466 Shavlakadze T, White J, Hoh JF, Rosenthal N, Grounds MD (2004) Targeted expression of insulin-like
467 growth factor-I reduces early myofiber necrosis in dystrophic mdx mice. Mol Ther 10(5):829–843.

468 Snow MH (1977) Myogenic cell formation in regenerating rat skeletal muscle injured by mincing. II. An
469 autoradiographic study. Anat Rec 188(2):201–217.

470 Snow MH (1978) An autoradiographic study of satellite cell differentiation into regenerating myotubes
471 following transplantation of muscles in young rats. Cell Tissue Res 186(3):535–540.

472 Stedman HH, Sweeney HL, Shrager JB, Maguire HC, Panettieri RA, Petrof B, Narusawa M, Leferovich
473 JM, Sladky JT, Kelly AM (1991). The mdx mouse diaphragm reproduces the degenerative changes of
474 Duchenne muscular dystrophy. Nature 352(6335):536–539.

475 Tedesco FS, Dellavalle A, Diaz-Manera J, Messina G, Cossu G (2010) Repairing skeletal muscle:

regenerative potential of skeletal muscle stem cells. J Clin Invest 120(1):11–19. doi: 10.1172/JCI40373

Ten Broek RW, Grefte S, Von den Hoff JW (2010) Regulatory factors and cell populations involved in skeletal muscle regeneration. J Cell Physiol 224(1):7–16. doi: 10.1002/jcp.22127

Tidball JG (2005) Inflammatory processes in muscle injury and repair. Am J Physiol Regul Integr Comp Physiol 288(2):R345–R353.

Tsivitse S (2010) Notch and Wnt signaling, physiological stimuli and postnatal myogenesis. Int J Biol Sci 6(3):268–281.

Walden DL, McCutchan HJ, Enquist EG, Schwappach JR, Shanley PF, Reiss OK, Terada LS, Leff JA, Repine JE (1990) Neutrophils accumulate and contribute to skeletal muscle dysfunction after ischemia-reperfusion. Am J Physiol 259(6 Pt 2):H1809–H1812.

Weller B, Karpati G, Carpenter S (1990) Dystrophin-deficient mdx muscle fibers are preferentially vulnerable to necrosis induced by experimental lengthening contractions. J Neurol Sci 100(1-2):9–13.

Zacks SI, Sheff MF (1982) Age-related impeded regeneration of mouse minced anterior tibial muscle. Muscle Nerve 5(2):152–161.

Figure Legends

Fig. 1 Age-dependent changes in phenotypes of B10 and mdx mice.

(**A**) Comparison of body weights between B10 and mdx mice. Values = mean ± SE. B10: n ≥ 4; mdx: n ≥ 10. *: $P < 0.01$ vs B10 at same age, Mann-Whitney *U*-test.

(**B**) Transverse sections of triceps brachii muscle from B10 and mdx mice stained with Masson's trichrome stain at 4 and 6 weeks of age. Bars = 1 mm (low magnification), 100 μm (high magnification).

Fig. 2 Comparison of myofibers between B10 (left) and mdx mice (right).

Transverse sections of triceps brachii muscle (TB) and costal part of the diaphragm (CPD) stained with Masson's trichrome stain at 6 weeks of age. Squared areas within low magnification images are

magnified in the right panels. B10 mice show no histopathological change in either TB or CPD. In mdx mice, degenerative myofibers (arrows, magnified panel of TB) are characterized by faint-colored and disrupting myofibers. Regenerating myofibers (small arrowheads, magnified panel of TB) are small and basophilic myofibers with central nuclei. Regenerated myofibers (large arrowheads, magnified panel of TB and CPD) have eosinophilic large myofibers and non-peripheral (including central) nuclei in mdx mice. Bars = 100 μm (low magnification), 20 μm (high magnification). w: weeks of age.

Fig. 3 Regenerative features of skeletal muscle lesions in mdx mice.

Transverse sections of the same area of triceps brachii muscle in mdx mice at 4 weeks of age. Hematoxylin and eosin staining (**A, D, G, and J**) and immunohistochemical staining for embryonic myosin heavy chain (eMyHC) (B, E, H, and K) and paired box 7 (PAX7) (**C, F, I, and L**). Numerous PAX7-positive muscle satellite cells surround eMyHC-positive regenerating myofibers in skeletal muscles of mdx mice (**A–F**), and the number of the former and the staining intensity of the latter gradually decrease with progression of myofiber regeneration (**A–C and G–L**). Bars = 100 μm (low magnification), 20 μm (high magnification).

Fig. 4 Ratio of degenerative and regenerative myofibers in skeletal muscles in mdx mice.

Myofibers classified into normal myofibers (**A**), degenerative myofibers (**B**), centronucleated myofibers (**C**), regenerating myofibers (**D**), or regenerated myofibers (**E**). The sum of values of regenerating myofibers and regenerated myofibers indicates the values of centronucleated myofibers. CT, cranial tibial muscle; GA, gastrocnemius muscle; QR, quadriceps femoris muscle; TB, triceps brachii muscle; LL, lumbar longissimus muscle; CPD, costal part of the diaphragm. Statistically significant differences among muscles from mice of the same age are indicated by different letters (C, G, Q, T, and D indicating CT, GA, QR, TB and CPD, respectively). Significant age differences between samples of the same muscle are indicated by symbols (* and†). Analyses were performed using Kruskal-Wallis test, followed by Scheffé's

method for multiple comparisons when a significant difference is observed ($P < 0.05$). Values = mean ± SE; 4 w, n = 4; 6 w and 14 w, n = 3. w: weeks of age

Fig. 5 Infiltration of immune cells in skeletal muscle lesions in mdx mice.

(**A–D**) Immunohistochemical staining for Iba1, Gr1, B220, and CD3 in triceps brachii muscle of mdx mice at 6 weeks of age. Bars: 100 μm (panels), 20 μm (insets).

(**E–H**) Comparison of the number of inflammatory cells in each skeletal muscle for mice at different ages. See Figure 4 legend for abbreviations. Statistically significant differences among muscles from mice of the same age are indicated by different letters (C, G, Q, T, and D indicating CT, GA, QR, TB, and CPD, respectively). Significant age differences between samples of the same muscle are indicated by symbols (* and†). Analyses were performed using Kruskal-Wallis test, followed by Scheffé's method for multiple comparisons when a significant difference was observed ($P < 0.05$). Values = mean ± SE. 4 w, n = 4; 6 w and 14 w, n = 3. w: weeks of age

Fig. 6 Correlation between inflammatory cell infiltration and ratio of degenerating, regenerating, and regenerated myofibers in mdx mice.

Graph showing Spearman's rank correlations between the density of inflammatory cells (Iba1: a-c, Gr1: d-f, B220: g-i, and CD3: j-l) and the ratio of degenerating (a, d, g and j), regenerating (b, e, h and k), and regenerated (c, f, i and l) myofibers.*: $P < 0.05$, Spearman's rank correlation test; ρ: Spearman's rank correlation coefficient. n = 29.

547 **Table 1** Antibodies, working dilutions, and methods for antigen retrieval

Antibody	Source	Dilution	Antigen retrieval	Heating condition
Mouse anti-eMyHC	DSHB (Iowa, USA)	1:900	20 mM Tris-HCl (pH 9.0)	105°C, 20 minutes
Mouse anti-PAX7	DSHB (Iowa, USA)	1:200	20 mM Tris-HCl (pH 9.0)	105°C, 20 minutes
Rabbit anti-Iba1	Wako (Osaka, Japan)	1:2000	0.1% pepsin/ 0.2 N HCl	37°C, 5 minutes
Rat anti-Gr1	R and D system (Minneapolis, USA)	1:800	0.1% pepsin/ 0.2 N HCl	37°C, 5 minutes
Rat anti-B220	Cedarlane (Ontario, Canada)	1:1600	20 mM Tris-HCl (pH 9.0)	105°C, 20 minutes
Rabbit anti-CD3	Nichirei (Tokyo, Japan)	1:500	20 mM Tris-HCl (pH 9.0)	105°C, 20 minutes

Fig. 1 Age-dependent changes in phenotypes of B10 and mdx mice.

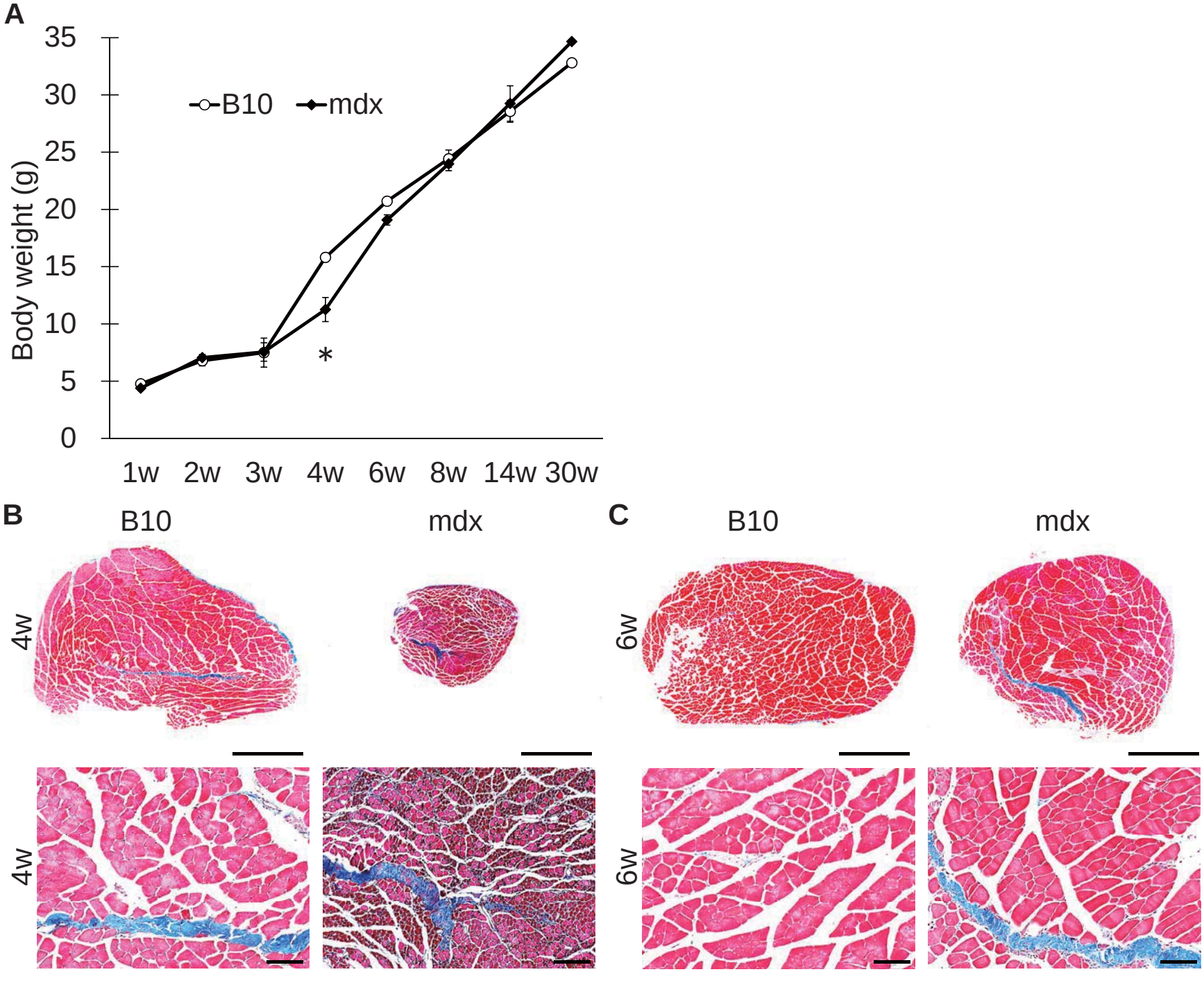

Fig. 2 Comparison of myofibers between B10 (left) and mdx mice (right).

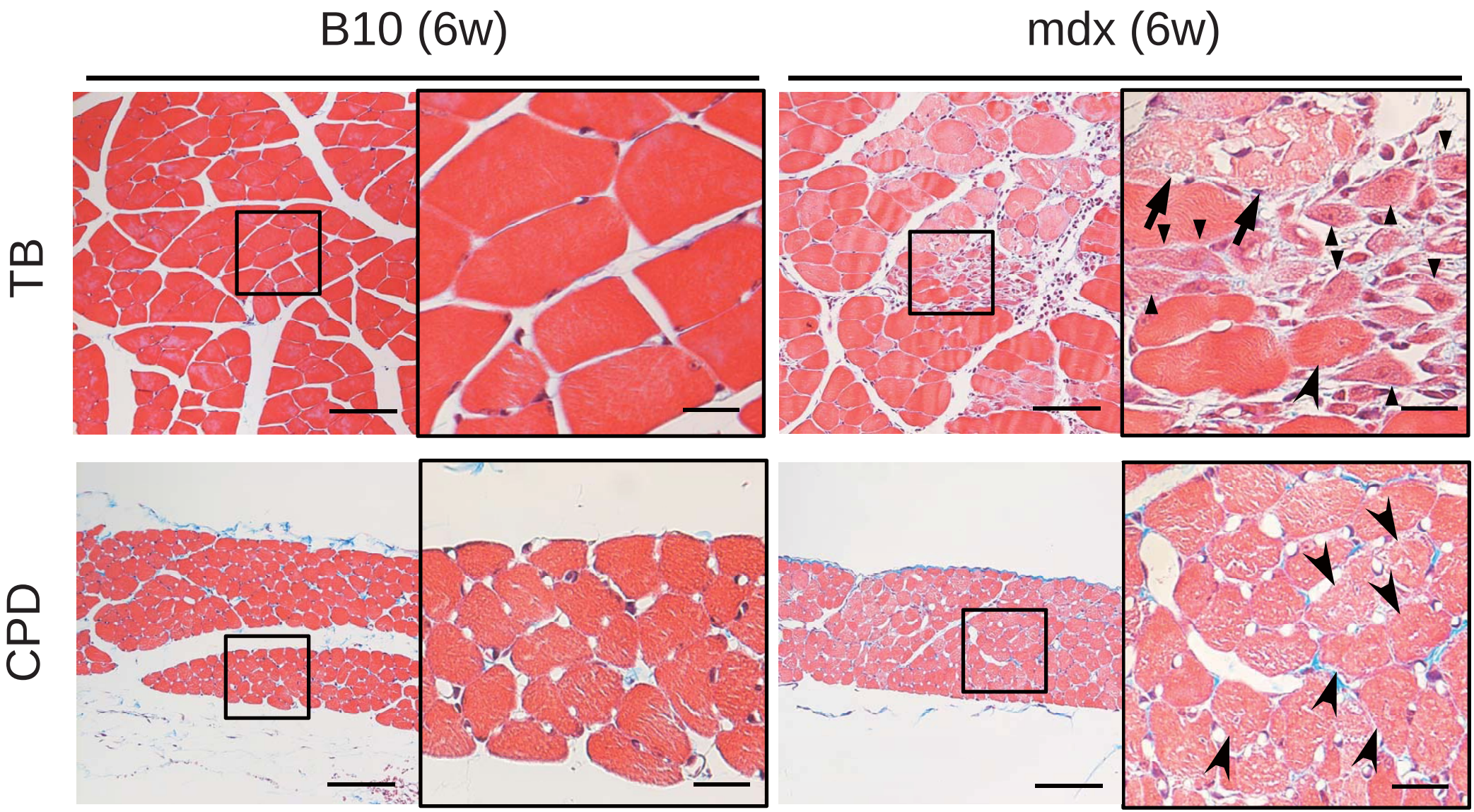

Fig. 3 Regenerative features of skeletal muscle lesions in mdx mice.

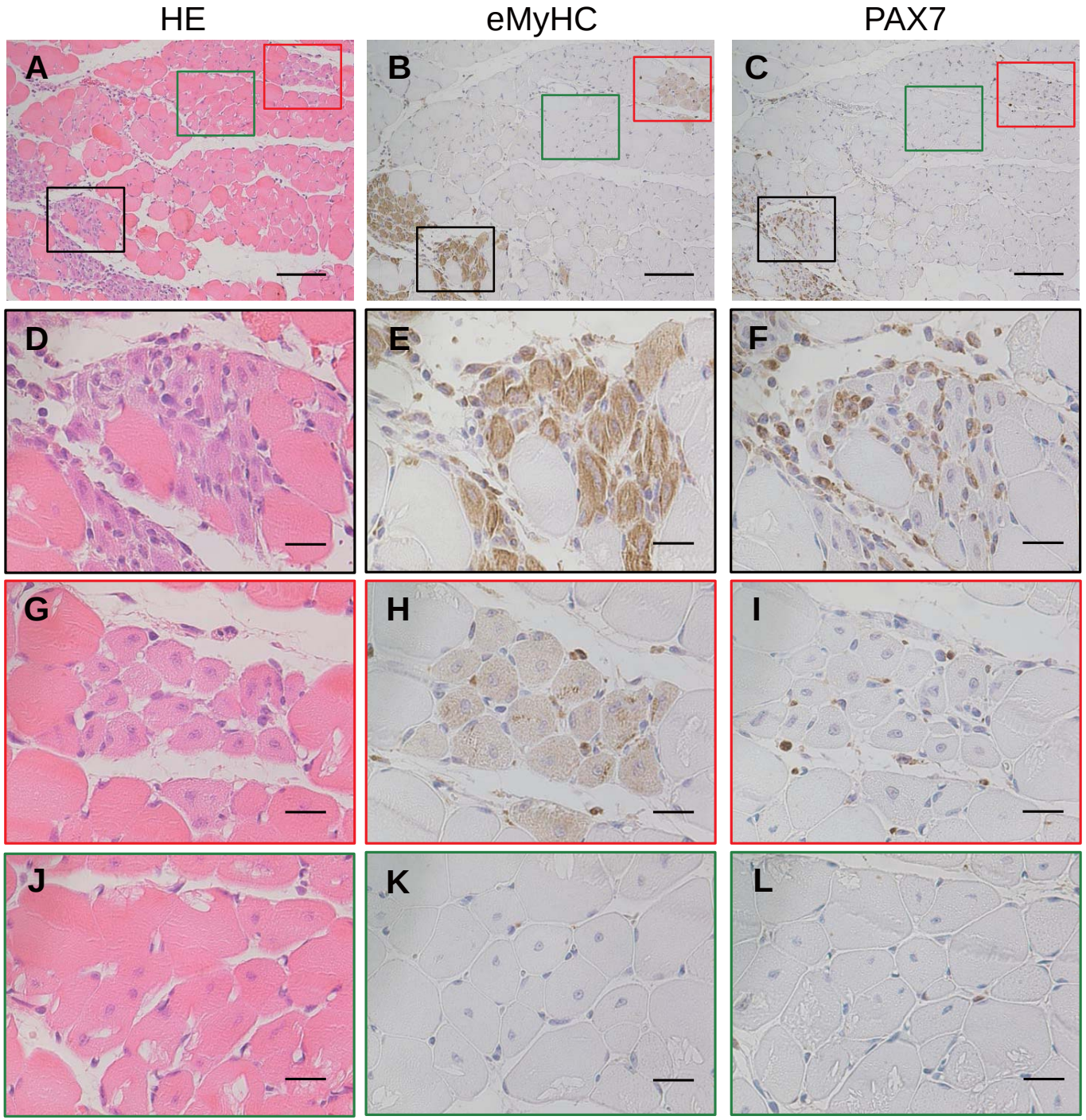

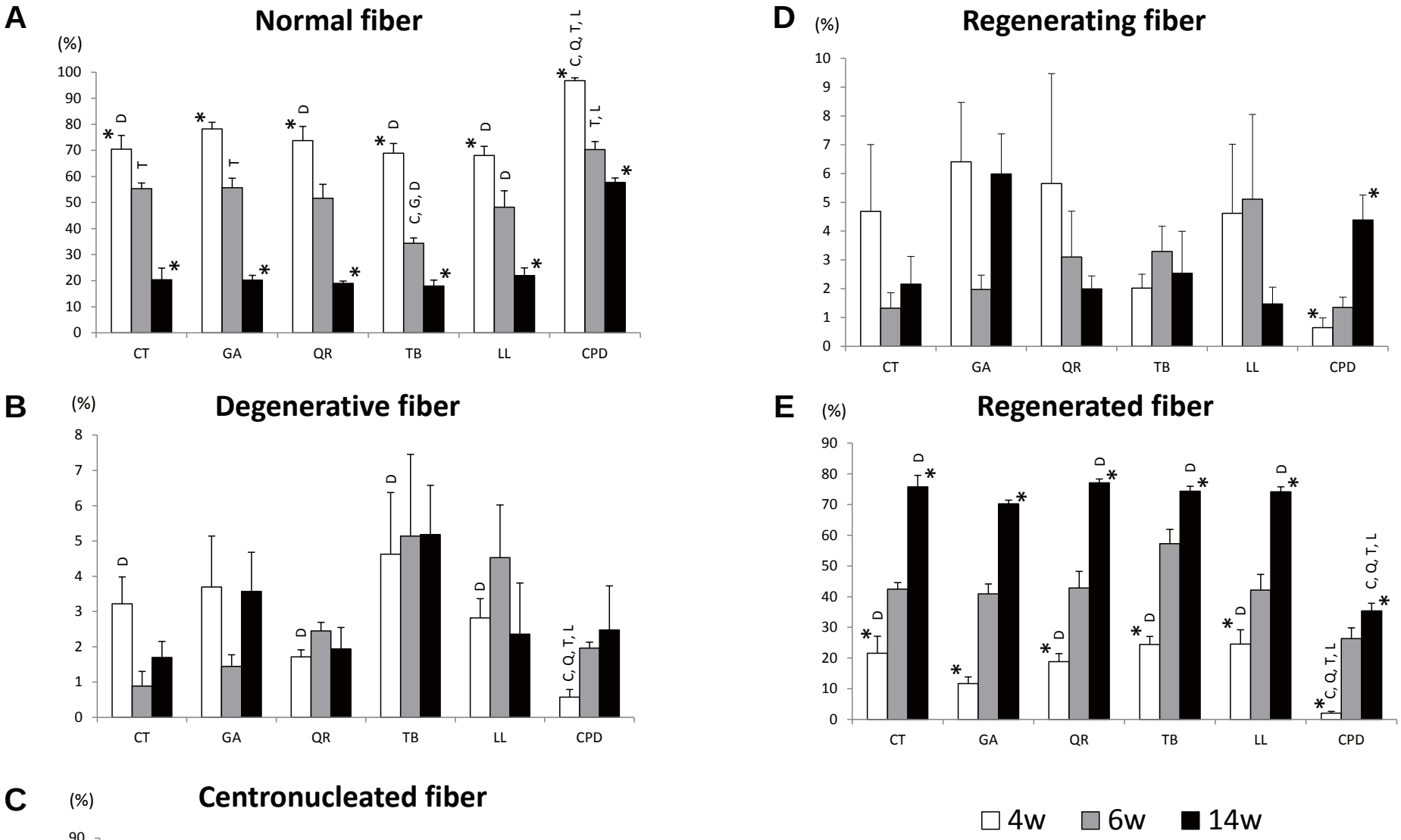

Fig. 4 Ratio of degenerative and regenerative myofibers in skeletal muscles in mdx mice.

Fig. 5 Infiltration of immune cells in skeletal muscle lesions in mdx mice.

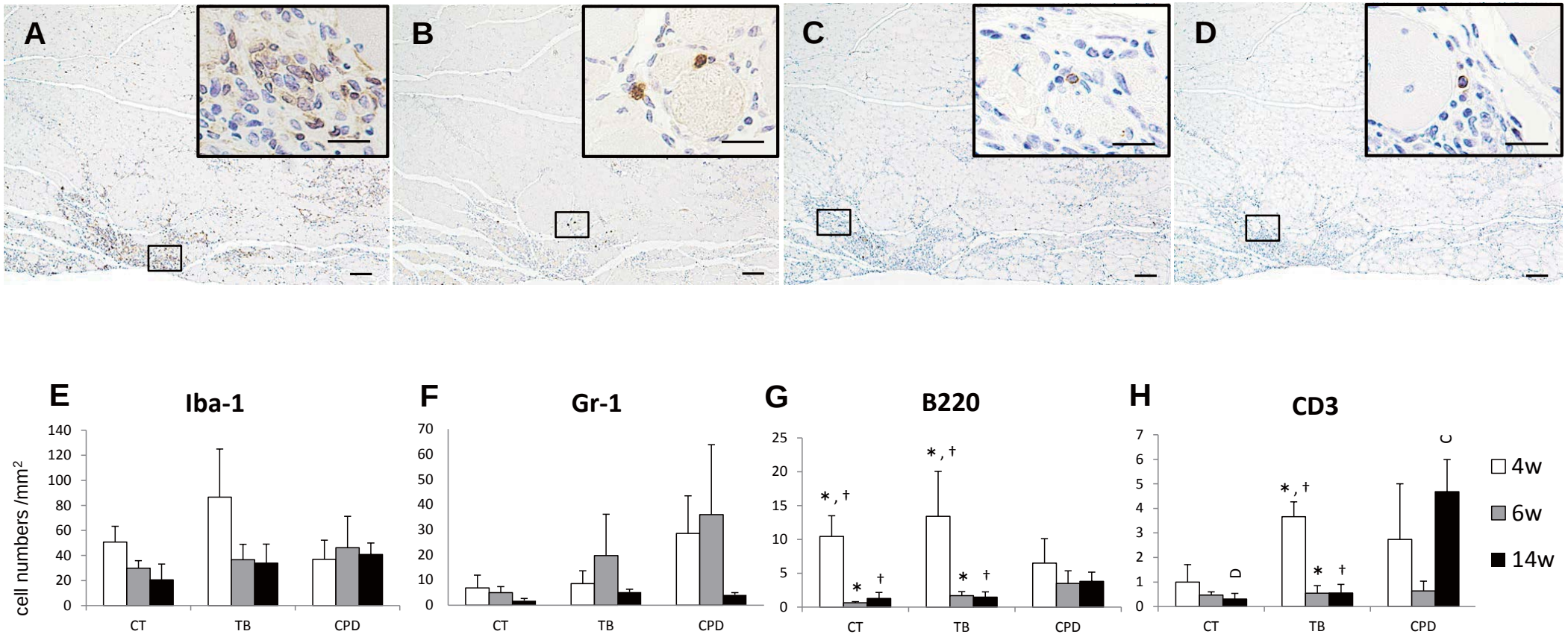
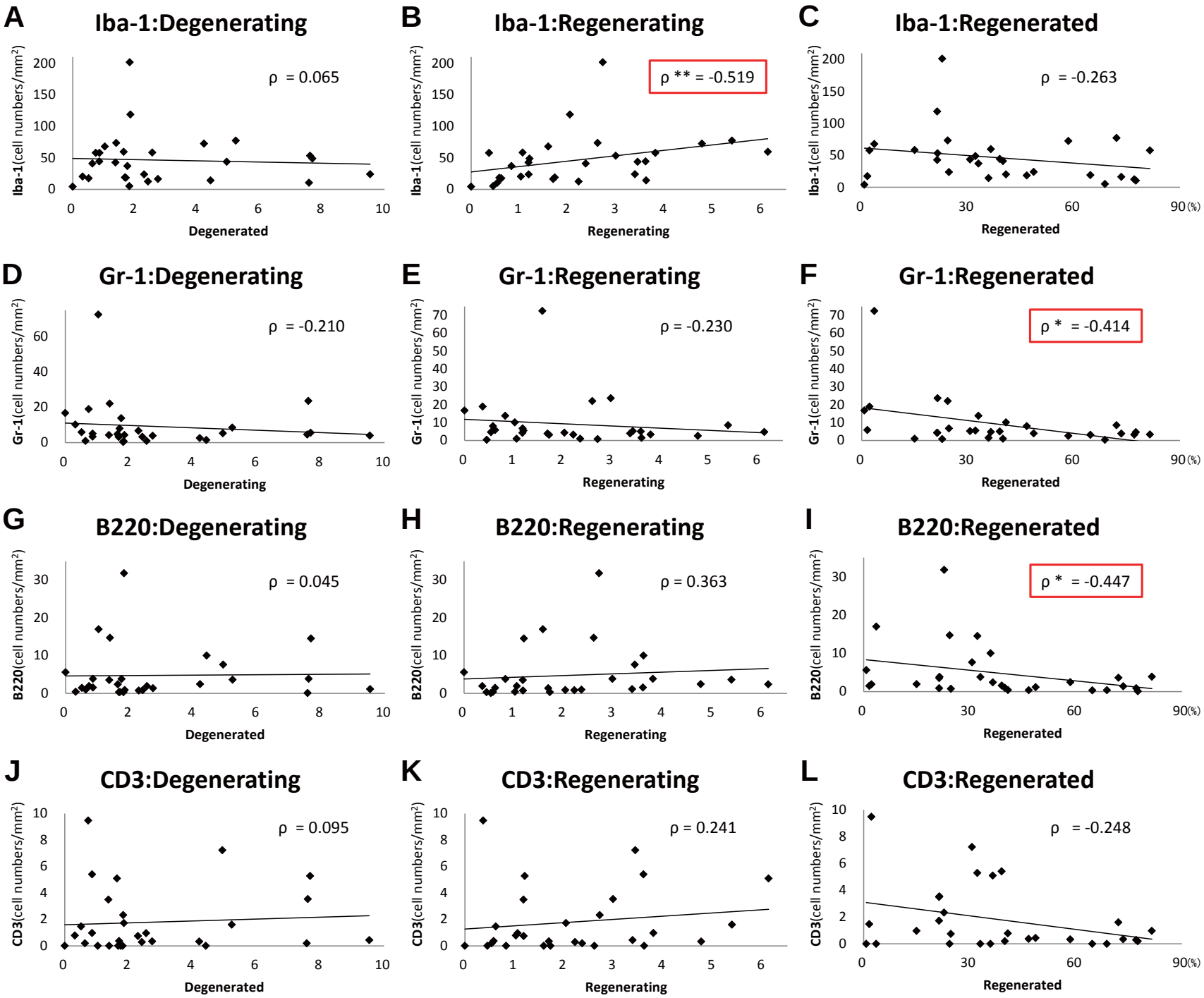
Fig. 6 Correlation between inflammatory cell infiltration and ratio of degenerating, regenerating, and regenerated myofibers in mdx mice.